

Token Transformer: Can class token help window-based transformer build better long-range interactions?

Jiawei Mao Yuanqi Chang Xuesong Yin *

School of Media and Design, Hangzhou Dianzi University, Hangzhou, China

{jiaweima0,211330020,yinxs}@hdu.edu.cn

Abstract

Compared with the vanilla transformer, the window-based transformer offers a better trade-off between accuracy and efficiency. Although the window-based transformer has made great progress, its long-range modeling capabilities are limited due to the size of the local window and the window connection scheme. To address this problem, we propose a novel Token Transformer (TT). The core mechanism of TT is the addition of a Class (CLS) token for summarizing window information in each local window. We refer to this type of token interaction as CLS Attention. These CLS tokens will interact spatially with the tokens in each window to enable long-range modeling. In order to preserve the hierarchical design of the window-based transformer, we designed Feature Inheritance Module (FIM) in each phase of TT to deliver the local window information from the previous phase to the CLS token in the next phase. In addition, we have designed a Spatial-Channel Feedforward Network (SCFFN) in TT, which can mix CLS tokens and embedded tokens on the spatial domain and channel domain without additional parameters. Extensive experiments have shown that our TT achieves competitive results with low parameters in image classification and downstream tasks.

1. Introduction

In recent years, Vision Transformer (ViT) [9] has relied on attention mechanisms for global contextual modeling and its own architecture to achieve success in various vision tasks. Compared with Convolutional Neural Network (CNN), various ViT improvement efforts [3, 5, 10, 11, 17, 18, 22, 23, 25–28, 31, 32, 40] have achieved results that can compete with them on multiple datasets. Although ViT performs well in computer vision, the secondary computational complexity caused by attention leads to the huge computational overhead of ViT. This has hindered the further devel-

*Corresponding author.

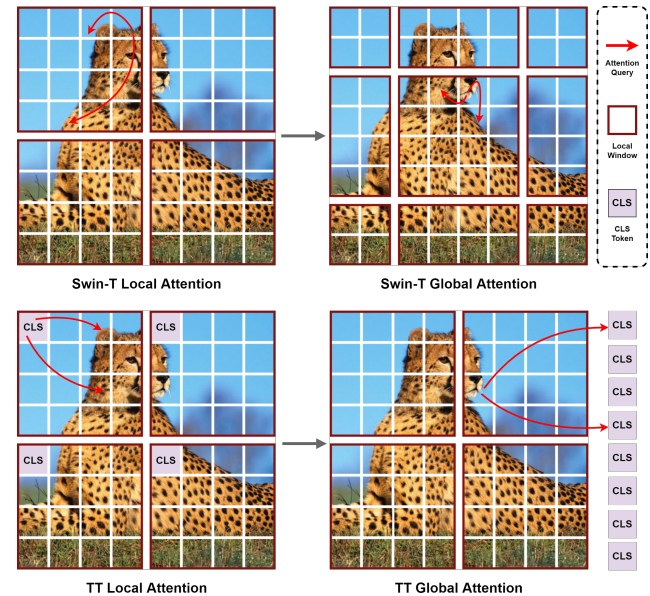


Figure 1. Compare Swin-T’s token interaction with TT. Swin-T enables long-range interaction between tokens through a window shift operation. However, the size of the window and the shift scheme limit its ability to interact at a distance. Our TT establishes efficient long-range dependency modeling while preserving the benefits of Swin-T by making CLS tokens capture window global information and making the tokens in each window interact with CLS tokens.

opment of ViT.

Some recent work has begun to try to address this issue. Wang et al [30]. introduced the pyramidal architecture of CNN into ViT to alleviate the problem of huge computation of ViT by reducing the resolution in a hierarchical way. Yin et al [36]. studied unimportant tokens in ViT and greatly reduced the throughput of the model by suspending unimportant tokens. Although these works have made good progress, the Swin Transformer (Swin-T) [20] proposed by Liu et al. achieves a better tradeoff between accuracy and efficiency through window attention as well as window shift

operations. However, the window size and window shift operations limit the long-range dependency modeling of the transformer. This in turn impairs the model performance.

In order to address the above issue, a QnA [1] layer is designed by introducing a trainable cross-window shared Query to further improve the expression of window-based transformer attention mechanisms by means of displacement invariance. Xia et al. proposed Deformable Attention Transformer (DAT) [33], which indirectly improves the model modeling capability by selecting more meaningful key-value pairs based on the data. Yang et al. [35] effectively captured short- and long-range visual dependencies by investigating new attention mechanisms that combine fine-grained local and coarse-grained global interactions.

While these efforts have slightly improved window-based transformer modeling capabilities, they require the addition of additional layers or large overhead operations. So in this paper, we propose a novel Token Transformer (TT) to solve the above problem. The key innovation of TT is CLS Attention, which introduces a CLS token for each window. The success of ViT and MoCo v3 [4] has demonstrated that CLS tokens already have the effect of summarizing global information by interacting spatially with embedded tokens. Inspired by these works, we introduce a CLS token in each window to represent the information of each window by way of window attention. The CLS token containing the window information will be used as the query to interact spatially with the token between each window by cross-attention, thus enabling efficient long-range dependency modeling. Hence, we do not need to introduce additional layers or complex computational operations. Fig. 1 shows the token interaction of TT compared with Swin-T. However, window-based transformers often use a layered design, which inevitably leads to a change in the number of windows and thus we need to create new CLS tokens when layering. In order to enable new CLS tokens to access the information contained in the previous CLS token, we design a Feature Inheritance Module (FIM) at each stage. It aggregates the previous stage CLS tokens by convolution and fuses the two stages of CLS tokens by spatial mixing. Besides, we design a simple and effective feedforward network in TT. We refer to the feedforward network in TT as Spatial-Channel Feedforward Network (SCFFN). In SCFFN, we perform token mixing not only on the spatial domain using Multi-Layer Perception (MLP), but also on the channel domain by convolution. This approach also introduces the inductive bias property of convolution for TT. And we do not increase the number of parameters of the feedforward network because we replaced the second layer of the conventional FFN network MLP with a 1x1 convolution. Such a feedforward network design is intuitive and simple, and helps us to enhance the ability to model the network over the channel domain.

We have conducted experiments to verify the effectiveness of TT. TT achieves competitive results on image classification task on ImageNet-1k [6], semantic segmentation task on ADE20K [39], and object detection task on CoCo [19] with fewer parameters.

In general, our main contributions are shown below:

- We designed a new long-distance dependency interaction called CLS Attention by introducing CLS tokens for each window. This interaction does not require the addition of additional layers or expensive computational operations, thus making the model lightweight and efficient. Based on this interaction, we have designed a novel transformer called TT, which has achieved competitive results in multiple visual tasks.
- To preserve the hierarchical design of window-based transformer, we designed the FIM for efficient message delivery of CLS tokens at different stages.
- We designed a novel feedforward network SCFFN in TT. SCFFN enhances the modeling capability of TT simply and intuitively without introducing additional parameters by using spatial channel token mixture implemented by MLP and convolution, respectively.

2. Related Work

2.1. ViT and its variants

The emergence of ViT [9] has successfully migrated the mainstream architecture transformer in Natural Language Processing (NLP) to the field of computer vision. ViT and its improvements has successfully outperformed or rivaled CNNs in several vision tasks with its global modeling capabilities. Zhou et al. [40] found that the transformer quickly saturates at deeper levels. Therefore, they proposed the Re-attention model in DeepViT to regenerate the attention map to enhance the diversity among layers with little computational cost. CrossViT [3] proposes a dual-branch transformer module to combine image patches of different sizes to produce stronger image features to improve the image classification performance of ViT. However, the secondary computational complexity associated with global modeling has affected the development of ViT. To solve this problem, Yuan et al. [38] proposed T2T by incorporating the experience of CNN architecture design. With its narrow and deep network design, T2T further improves the performance of ViT while reducing the number of ViT parameters. CCT [13] proposes self-attention processing using convolution rather than direct image chunking. This allows CCT to have higher accuracy and fewer parameters. PiT [15] combines a pooling layer with a transformer architecture to reduce the model computation in a way that reduces the space size. CvT [32] improves the performance and efficiency of ViT by introducing convolution into ViT to produce the best re-

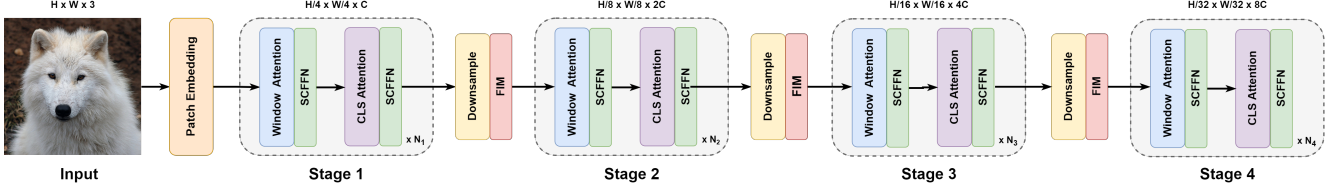


Figure 2. TT’s overall pipeline. N_1 to N_4 represent the number of token transformer modules in each stage, respectively.

sults of both designs. Wang et al. [30] further improved the efficiency of ViT by transforming it into a PVT with a pyramidal architecture. RegionViT [2] uses a novel Regional-to-Local Attention instead of Global Self-Attention in ViT to reduce the computational effort. AViT [36] introduces a pause probability for each layer of embedded tokens, improving ViT efficiency by reducing unimportant token interactions.

2.2. Window-based transformer

Swin transformer [20] succeeds in reducing the secondary computational complexity of ViT to linear with its window-based attention design and window shift operation. With these careful designs, Swin-T perfectly achieves the trade-off between accuracy and computational volume. Despite these excellent results, its long-range modeling capability is somewhat impaired by the limitations of the window size and shift operations. To address this issue, Dong et al. [8] developed the Cross-Shaped Window self-attention mechanism for computing self-attention in parallel in the horizontal and vertical stripes that form the cross-shaped window. This design achieves a powerful modeling capability while limiting the computational cost. Xie et al. [33] proposed DAT to solve this problem by finding the most relevant key-value pairs based on the intrinsic relationship of the data. Focal Transformer [35] enhances network modeling capabilities by designing complex coarse-grained local and fine-grained global interaction mechanisms. Li et al. [16] proposed a multi-branch, multi-scale Self-Attention-aware approach to LG-Transformer indirectly enhancing the modeling capability of Swin-T. MOA-Transformer [24] designs multi-resolution overlapping attention modules to generate global features. Arar et al. [1] designed window-shared learnable query for window-based transformer to introduce convolutional locality and variability to improve the expressiveness of the attention mechanism. Ding et al. [7] designed Channel Group Attention, which allows their DaViT to model the global space at the channel level with linear computational complexity. In addition Wang et al. [29] introduced convolutional embeddings for each transformer module to improve the modeling ability of hierarchical vision transformers such as swin-T, Cswin-T. Inspired by the dilated convolution [37], Hassani et al. [12] proposed Dilated Neighborhood Attention, which addresses

the lack of Swin’s ability to model long-range dependencies by expanding the receptive field.

3. Method

3.1. Preliminaries

We first review the attention mechanism in swin transformer [20]. Swin-T mainly adopts window based multi-head self-attention (W-MSA) mechanism and shifted window based multi-head self-attention (SW-MSA) mechanism. Given an input image $x \in R^{H \times W \times 3}$, the patch splitting module splits it into non-overlapping patches. The linear embedding layer will project them as sequential patches $x_p \in R^{N \times C}$, where H and W are the height and width of the input image, $C = p^2e$, p denotes the patch size, e denotes the embedding dimension, and $N = HW/p^2$ denotes the number of patches. Assume that each local window contains M patches $z \in R^{M \times C}$. W-MSA performs multi-head attention on the patches in each window separately. The W-MSA with N heads is specified as

$$\begin{aligned} q &= zW_q, k = zW_k, v = zW_v, \\ o^{(n)} &= \theta(q^{(n)}k^{(n)T}/\sqrt{d} + B)v^{(n)}, n = 1, \dots, N, \\ o &= [o^{(1)}, \dots, o^{(N)}]W_o, \end{aligned} \quad (1)$$

In Eq. (1), W_q, W_k, W_v, W_o represents the mapping matrix. $\theta(\cdot)$ is the softmax function, $d = C/N$ is the embedding dimension of each header and $B \in R^{N \times N}$ is the relative position bias. $[\cdot]$ means Concat operation. Next, each window is shifted and then the W-MSA calculation is performed once again, resulting in a long-range dependency modeling, also known as SW-MSA. Overall, the attention mechanism of Swin-T is calculated as

$$\begin{aligned} \hat{o}^l &= \text{W-MSA}(\text{LN}(o^{l-1})) + o^{l-1}, \\ o^l &= \text{MLP}(\text{LN}(\hat{o}^l)) + \hat{o}^l, \\ \hat{o}^{l+1} &= \text{SW-MSA}(\text{LN}(o^l)) + o^l, \\ o^{l+1} &= \text{MLP}(\text{LN}(\hat{o}^{l+1})) + \hat{o}^{l+1}, \end{aligned} \quad (2)$$

where $\text{LN}(\cdot)$ denotes Layer Normalization.

3.2. Overall Architecture

Fig. 2 illustrates the overall architecture of TT. TT mainly consists of patch embed layer, token transformer

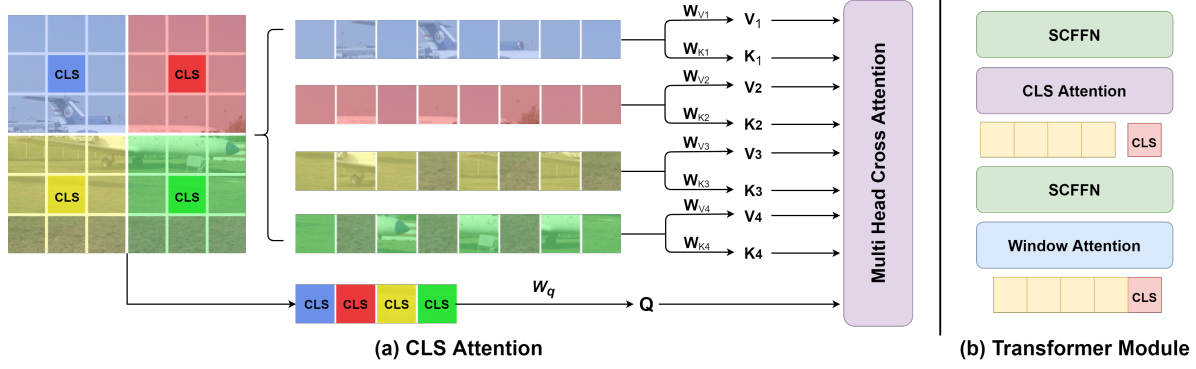


Figure 3. (a) illustrates the CLS Attention mechanism. The CLS token first captures local window information through window attention. The area with the same color as the CLS token indicates the receptive field of the CLS token. Then, all CLS tokens are projected as queries, and the tokens in each window are projected as keys and values respectively. All keys and values share the same query. Eventually, long-range dependency modeling is achieved by multi head cross attention. (b) describes the internal construction of the token transformer module.

module and feature inheritance module. The model architecture remains a hierarchical design. Each stage reduces the feature map resolution by a factor of two. For the input image x , we divide it into non-overlapping patches and project these patches by a patch embedding layer composed of convolution. We then assign the patch to multiple non-overlapping local windows and add a CLS token to each window. Finally, we input the tokens from each window into the token transformer module for local and global modeling. In addition to downsampling during the layering phase, we also design the feature inheritance module for passing information from the previous phase window to the new CLS token.

3.3. Token Transformer Module

The token transformer module mainly consists of local window attention and global attention based on CLS tokens (CLS Attention). Besides, we design a Spatial-Channel Feedforward Network in the token transformer module which enhances network modeling capabilities in a simple and intuitive way. We show the CLS Attention of the token transformer module in Fig. 3.

CLS Attention For token $z \in R^{M \times C}$ in each window, we add a CLS token $\in R^{1 \times C}$ to it to get $\hat{z} \in R^{(M+1) \times C}$. For \hat{z} , we perform local modeling of window attention and make the CLS token aware of the local information of the window. The process is computing according to:

$$\begin{aligned} \hat{z} &= [\text{cls}, z], \\ \hat{z} &= \text{W-MSA}(\text{LN}(\hat{z})) + \hat{z}, \end{aligned} \quad (3)$$

In the next stage, we integrate CLS tokens from all windows and use them as queries for long-range dependency modeling. The CLS token will interact with the embedded tokens z in each local window, which will be used as key and value.

The whole interaction process is realized through the cross-attention mechanism. Eq. (4) illustrates this.

$$\begin{aligned} z_q &= [\text{cls}^{(1)}, \dots, \text{cls}^{(T)}], \\ q &= z_q W_q, k = z W_k, v = z W_v, \\ o^{(n)} &= \theta(q^{(n)} k^{(n)T} / \sqrt{d} + B) v^{(n)}, n = 1, \dots, N, \\ o &= [o^{(1)}, \dots, o^{(N)}] W_o, \end{aligned} \quad (4)$$

where T is the number of windows, $W_q \in R^{C \times C}$ is the mapping matrix of CLS tokens, and $W_k, W_v \in R^{C \times C}$ are the projection matrices of the embedded tokens in the windows. By cross-attention based on CLS tokens and embedded tokens in local windows, we have successfully implemented the modeling of long-range dependencies. We provide the pseudo-code for the pytorch version of TT implementing long-range interaction in Algorithm 1.

SCFFN. We propose a novel feedforward network without introducing additional parameters. In addition to retaining the spatial mixing function of the feedforward network, we have added a channel mixing mechanism to enhance the network modeling capability.

Given the embedding token z and the CLS tokens in all windows, SCFFN first performs spatial mixing on them by MLP and then transposes the dimensions to perform channel mixing. Generally, SCFFN are computed as

$$\begin{aligned} z &= \text{MLP}(\text{LN}(z)) + z, \\ z &= \text{Conv}(\text{LN}(\text{trans}(z))) + \text{trans}(z), \\ z &= \text{trans}(z), \\ \text{cls} &= \text{SCFFN}(\text{cls}), \\ o &= [\text{cls}, z], \end{aligned} \quad (5)$$

Algorithm 1 CLS Attention: PyTorch-like Pseudocode

```

class WindowAttentionGlobal(nn.Module):
    def __init__(
        self, dim, window_size, num_windows,
        attn_drop=0., proj_drop=0.):
        super().__init__()
        self.q = nn.Linear(dim, all_head_dim, bias=False)
        self.k = nn.Linear(dim, all_head_dim, bias=False)
        self.v = nn.Linear(dim, all_head_dim, bias=False)
        self.attn_drop = nn.Dropout(attn_drop)
        self.proj = nn.Linear(all_head_dim, dim)
        self.proj_drop = nn.Dropout(proj_drop)

    def forward(self, x):
        B_, N, C = x.shape
        B = int(B_ // self.num_windows)
        cls_token, token = x[:, :, 1:], x[:, :, 1:]
        cls_token = rearrange(cls_token, (b n) d c ->
            b n d c, b=B).repeat(1, 1, self.
                num_windows, 1)
        cls_token = rearrange(cls_token, b n d c -> (
            b d) n c)
        k = v = token
        q = cls_token
        N_k, N_v = k.shape[1], v.shape[1]
        q = F.linear(input=q, weight=self.q.weight)
        q = q.reshape(B, N, 1, self.num_heads, -1).
            permute(2, 0, 3, 1, 4).squeeze(0)
        k = F.linear(input=k, weight=self.k.weight)
        k = k.reshape(B, N_k, 1, self.num_heads, -1).
            permute(2, 0, 3, 1, 4).squeeze(0)
        v = F.linear(input=v, weight=self.v.weight)
        v = v.reshape(B, N_v, 1, self.num_heads, -1).
            permute(2, 0, 3, 1, 4).squeeze(0)
        attn = self.attn_drop((q @ k.transpose(-2,
            -1)).softmax(dim=-1))
        x = (attn @ v).transpose(1, 2).reshape(B, N,
            -1)
        x = self.proj_drop(self.proj(x))
        return x
  
```

Notes: num_windows indicates the number of windows. rearrange() is a shape change operation.

where $trans(\cdot)$ represents the dimension transpose operation, $Conv(\cdot)$ is the convolution operation with a convolution kernel of 1. Compared with the conventional FFN, we did not increase the number of parameters since we only replaced the MLP in its second layer using 1x1 convolution. However, this intuitive and simple feedforward design adds the benefits of convolutional inductive bias and channel modeling to TT, allowing for more sophisticated modeling.

3.4. Feature Inheritance Module

Since window-based transformers usually use a hierarchical design, this inevitably leads to a reduction in the number of windows and thus we need to design new CLS tokens at each stage. However, the new CLS token is missing the local window information of the previous resolution feature map and thus does not facilitate the use of multi-scale features. To solve this issue, we designed feature inheritance modules for passing CLS token information in each phase of TT. Fig. 4 shows the detailed flow of the FIM.

Specifically, supposing that all CLS tokens are a $T \times C$

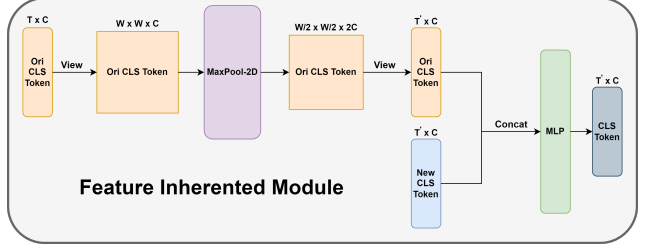


Figure 4. FIM architecture. We first divide the tokens into horizontal and vertical axis CLS tokens. Next, we downsample and integrate the horizontal and vertical axis CLS tokens through the max-pooling layer. We then merge the horizontal and vertical axis CLS tokens and combine them with the new CLS tokens by channel dimension. Ultimately we transfer information between the origin CLS tokens and new CLS tokens through the MLP layer.

matrix at a certain stage, FIM will first extend T to $H, W = \sqrt{T}$. H and W denote the number of horizontal and vertical CLS tokens in the feature map, respectively. Next, we perform a down-sampling operation on the CLS tokens $\in R^{H \times W \times C}$ by a 3×3 convolutional layer with stride of 2 and padding of 1. This step successfully integrates CLS tokens of the feature map in both horizontal and vertical directions and expands the embedding dimension of CLS tokens. Then FIM will transform the previous CLS tokens $\in R^{(H/2) \times (W/2) \times 2C}$ into the shape of the new CLS tokens and merge them by channel dimension. Finally, we use the projection matrix $W_c \in R^{4C \times 2C}$ to integrate the CLS tokens for the two stages. Algorithm 2 illustrates the pseudocode of FIM based on Pytorch.

Algorithm 2 FIM: PyTorch-like Pseudocode

```

class FeatureInheritanceModule(nn.Module):
    def __init__(self, dim, kernel_size=3, stride=2,
        pad=1):
        super(FeatureInheritanceModule, self).__init__()
        self.maxpool = nn.MaxPool2d(kernel_size=
            kernel_size, stride=stride, padding=pad)
        self.cls_mlp = nn.Linear(in_features=int(
            (dim // 2) * 3), out_features=dim, bias=False)

    def forward(self, ori_cls, new_cls):
        CB, CN, CC = new_cls.shape
        B, N, C = ori_cls.shape
        batch = CB
        Window = int(B // batch)
        W = int(Window ** 0.5)
        ori_cls = ori_cls.view(batch, C, W, W)
        ori_cls = self.maxpool(ori_cls)
        ori_cls = ori_cls.view(CB, CN, CC // 2)
        cls_token = torch.cat([ori_cls, new_cls], dim
            =-1)
        cls_token = self.cls_mlp(cls_token)
        return cls_token
  
```

3.5. Architecture Variants

We designed three different versions of Token Transformer according to the parameter size: TT-T, TT-S and

TT-B. The hyperparameters and network configurations for each version of Token Transformer are listed in Tab. 1.

TT Architectures			
	TT-T	TT-S	TT-B
Stage 1 (49 × 49)	$N_1 = 3, C = 64$ $W = 7, H = 2$	$N_1 = 4, C = 96$ $W = 7, H = 3$	$N_1 = 5, C = 128$ $W = 7, H = 4$
Stage 2 (25 × 25)	$N_2 = 4, C = 128$ $W = 5, H = 4$	$N_2 = 5, C = 192$ $W = 5, H = 6$	$N_2 = 6, C = 256$ $W = 5, H = 8$
Stage 3 (16 × 16)	$N_3 = 19, C = 256$ $W = 4, H = 8$	$N_3 = 21, C = 384$ $W = 4, H = 12$	$N_3 = 22, C = 512$ $W = 4, H = 16$
Stage 4 (9 × 9)	$N_4 = 5, C = 512$ $W = 3, H = 16$	$N_4 = 5, C = 768$ $W = 3, H = 24$	$N_4 = 5, C = 1024$ $W = 3, H = 32$

Table 1. Details of the configuration of TT and its variants. N represents the number of modules, C is the embedding dimension, W denotes the window size, and H refers to the number of attention heads.

4. Experiments

We perform image classification experiments with Token Transformer on ImageNet-1k [6], a object detection task on CoCo [19], and a semantic segmentation performance test on ADE20K [39]. Next, we verify the effectiveness of each important component of TT by ablation experiments on ImageNet-1k.

4.1. Image Classification on ImageNet-1K

Method	Resolution	#Params	#Flops	Top-1
Swin-T [20]	224 ²	29M	4.5G	81.3
ConvNeXt-T [21]	224 ²	29M	4.5G	82.1
Focal-T [35]	224 ²	29M	4.9G	82.2
PVT-S [30]	224 ²	24M	3.8G	79.8
ViT-Small [9]	224 ²	24M	5.1G	82.0
DAT-T [33]	224 ²	29M	4.6G	82.0
LG-T [16]	224 ²	32M	4.8G	82.1
QnA-Tiny [1]	224 ²	16M	2.5G	81.7
TT-T	224 ²	25M	3.9G	82.5
Swin-S [20]	224 ²	50M	8.8G	83.0
ConvNeXt-S [21]	224 ²	50M	8.7G	83.1
Focal-S [35]	224 ²	51M	9.1G	83.5
PVT-M [30]	224 ²	44M	6.9G	81.2
ViT-Medium [9]	224 ²	39M	9.1G	83.3
DAT-S [33]	224 ²	50M	9.0G	83.7
LG-S [16]	224 ²	61M	9.4G	83.3
QnA-Small [1]	224 ²	25M	4.4G	83.2
TT-S	224 ²	47M	7.7G	83.7
Swin-B [20]	224 ²	88M	15.5G	83.5
ConvNeXt-B [21]	224 ²	89M	15.4G	83.8
Focal-B [35]	224 ²	89M	16.0G	83.8
PVT-L [30]	224 ²	61M	9.8G	81.7
ViT-Base/16 [9]	224 ²	86M	17.6G	77.9
DAT-B [33]/16	224 ²	88M	15.8G	84.0
QnA-Base [1]	224 ²	56M	9.7G	83.7
TT-B	224 ²	86M	14.6G	84.2

Table 2. TT is compared with other state-of-the-art algorithms on ImageNet-1k for top-1 accuracy, parametric number size.

Settings. We pre-train and fine-tune TT on the ImageNet-1k dataset. The ImageNet-1k dataset consists of a training set of 1.28 million images and a validation set of 500,000 images. The dataset is divided into a total of 1000 categories. We test the performance of our three variants on ImageNet-1k and compared it with other transformer models.

All models are performed on 224 × 224 resolution images. We use the AdamW optimizer with an initial learning rate of 1e-4 for gradient updating. In addition, the model is trained with a total of 350 epochs and a weight decay of 0.05. The learning rate strategy employs a cosine decay scheduler with 20 warm-up and cool-down cycles. Moreover, we use most of the data enhancement strategies. All models are implemented in Nvidia RTX 3090.

Results. We provide the experimental results of image classification on ImageNet-1k in Tab. 2. We compare with current ViT, CNN, and window-based models. It is worth mentioning that our TT and its various variants achieve state-of-the-art classification performance with a small number of parameters and less computational complexity.

4.2. Object Detection on COCO

Method	#Params	#Flops	AP^b	AP_{50}^b	AP_{75}^b	AP^m	AP_{50}^m	AP_{75}^m
Swin-T [20]	48M	267G	46.0	68.1	50.3	41.6	65.1	44.9
ConvNeXt-T [21]	48M	262G	46.2	67.9	50.8	41.7	65.0	44.9
DAT-T [33]	48M	272G	47.1	69.2	51.6	42.4	66.1	45.5
TT-T	44M	245G	47.2	69.2	51.7	42.6	66.2	45.6
Swin-S [20]	69M	359G	48.5	70.2	53.5	43.3	67.3	46.6
DAT-S [33]	69M	378G	49.0	70.9	53.8	44.0	68.0	47.5
TT-S	66M	343G	48.9	70.7	53.7	44.1	68.0	47.4

Table 3. Comparison of TT with other models for object detection results on the CoCo dataset.

Settings. We use the CoCo dataset to evaluate the object detection performance of TT. The CoCo dataset consists of a training set of 118k images and a validation set of 5k images. We use TT and its variants trained on ImageNet-1k as Mask R-CNN [14] 3 x schedule backbone. We use the training settings of Swin-T for object detection training on CoCo.

Results. Tab. 3 shows the target detection results of TT and its three variants as well as several comparison algorithms on the CoCo dataset. We use Swin-T as a baseline and compare TT with various SOTA object detection algorithms such as CNN-based ConvNext [21] and window-based DAT [33]. The experiments show that TT and its various variants demonstrate competitive results for object detection on the CoCo dataset.

Backbone	Method	#Params	#Flops	mIoU
Swin-T [20]	UperNet	60M	945G	44.5
DAT-T [33]	UperNet	60M	957G	45.54
DeiT-Small/16 [26]	UperNet	52M	1099G	44.0
Focal-T [35]	UperNet	62M	998G	45.8
TT-T	UperNet	56M	883G	46.3
Swin-S [20]	UperNet	81M	1038G	47.6
DAT-S [33]	UperNet	81M	1079G	48.31
Focal-S [35]	UperNet	85M	1130G	48.0
TT-S	UperNet	78M	1006G	48.0
Swin-B [20]	UperNet	121M	1188G	48.1
DAT-B [33]	UperNet	121M	1212G	49.38
Focal-B [35]	UperNet	126M	1354G	49.0
TT-B	UperNet	117M	1151G	48.8

Table 4. Comparison of TT with other models for semantic segmentation results on the ADE20K dataset.

4.3. Semantic Segmentation on ADE20K

Settings. ADE20K is an accepted standard dataset for semantic segmentation tasks. It contains 20K training images and 2K validation images. In the semantic segmentation task, we still use the pre-training weights of TT on ImageNet-1k, and use UperNet [34] as the segmentation head. For a fair comparison, we still keep the same training settings as Swin-T in the semantic segmentation task.

Results. We present the results of TT compared with various SOTA models in Tab. 4. It contains the number of model parameters and the mIoU metric for the semantic segmentation task. We still choose Swin-T as the baseline and select DeiT, Focal and DAT for comparison. Compared with other models, TT still achieves competitive results with fewer parameters, which demonstrates the effectiveness of TT in the semantic segmentation task.

4.4. Ablation Study

In this section, we verify their validity by ablating important components of TT through image classification experiments on ImageNet-1k. We next report their ablation results in detail.

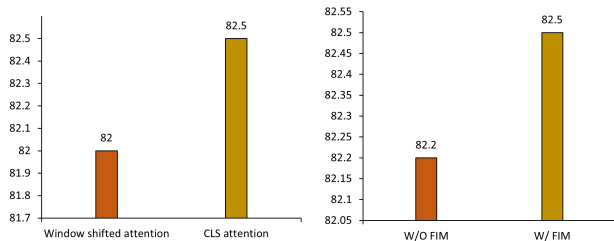


Figure 5. CLS Attention ablation results. Figure 6. FIM ablation results.

CLS Attention. We first verify the effectiveness of CLS Attention based on CLS tokens. Specifically, while we add CLS tokens to each local window, we eliminate the use of

cross-attention for remote interaction between CLS tokens and embedded tokens in the local window. Instead, we use a shift window approach for long-range dependency modeling. As shown in Tab. 5, the Top-1 accuracy of image classification on ImageNet-1k with TT using shift operation decreased by 0.5 compared to the remote attention mechanism based on CLS token. This demonstrates the effectiveness of our proposed Long-range attention mechanism based on CLS token to capture global information.

Spatial-channel feedforward network. For the ablation experiments of the spatial-channel feedforward network, we investigate the effectiveness of SCFFN acting on CLS tokens and embedded tokens. Specifically, we designed three classification experiments for testing using conventional feedforward networks instead of SCFFN without considering the number of parameters. If only SCFFN is used for CLS tokens and FFN is used for embedded tokens, the top-1 accuracy of TT-T decreases by 0.2. If only FFN is used for CLS tokens and SCFFN is used for embedded tokens, the classification experiment of TT-T crashes. If FFN is used for both CLS token makes and embedded tokens, the top-1 accuracy of TT-T decreases by 0.3. The specific results are detailed in Fig. 5. This indicates that SCFFN is more useful for CLS tokens and it enhances the modeling capability of TT more than the normal feedforward network.

Backbone	CLS token	Embed token	Top-1 acc
TT-T	FFN	FFN	82.2(-0.3)
	SCFFN	FFN	82.3(-0.2)
	FFN	SCFFN	-
	SCFFN	SCFFN	82.5

Table 5. Ablation studies of SCFFN on TT-T.

Feature Inheritance Module. Finally, we investigate whether the messaging of CLS tokens at different stages is effective. Specifically, we remove the feature inheritance modules in different phases and provide only new CLS tokens for each phase. Fig. 6 shows the ablation results of FIM for image classification on ImageNet-1k. The results show that removing FIM decreases the Top-1 accuracy by 0.3. This result illustrates the importance of FIM for TT to model long-range dependencies using multi-scale features.

4.5. Visualization

To demonstrate the performance of CLS Attention, we show the results of TT last layer attention visualization on the ImageNet-1k dataset. Fig. 7 shows the TT focused areas of interest in various types of images.

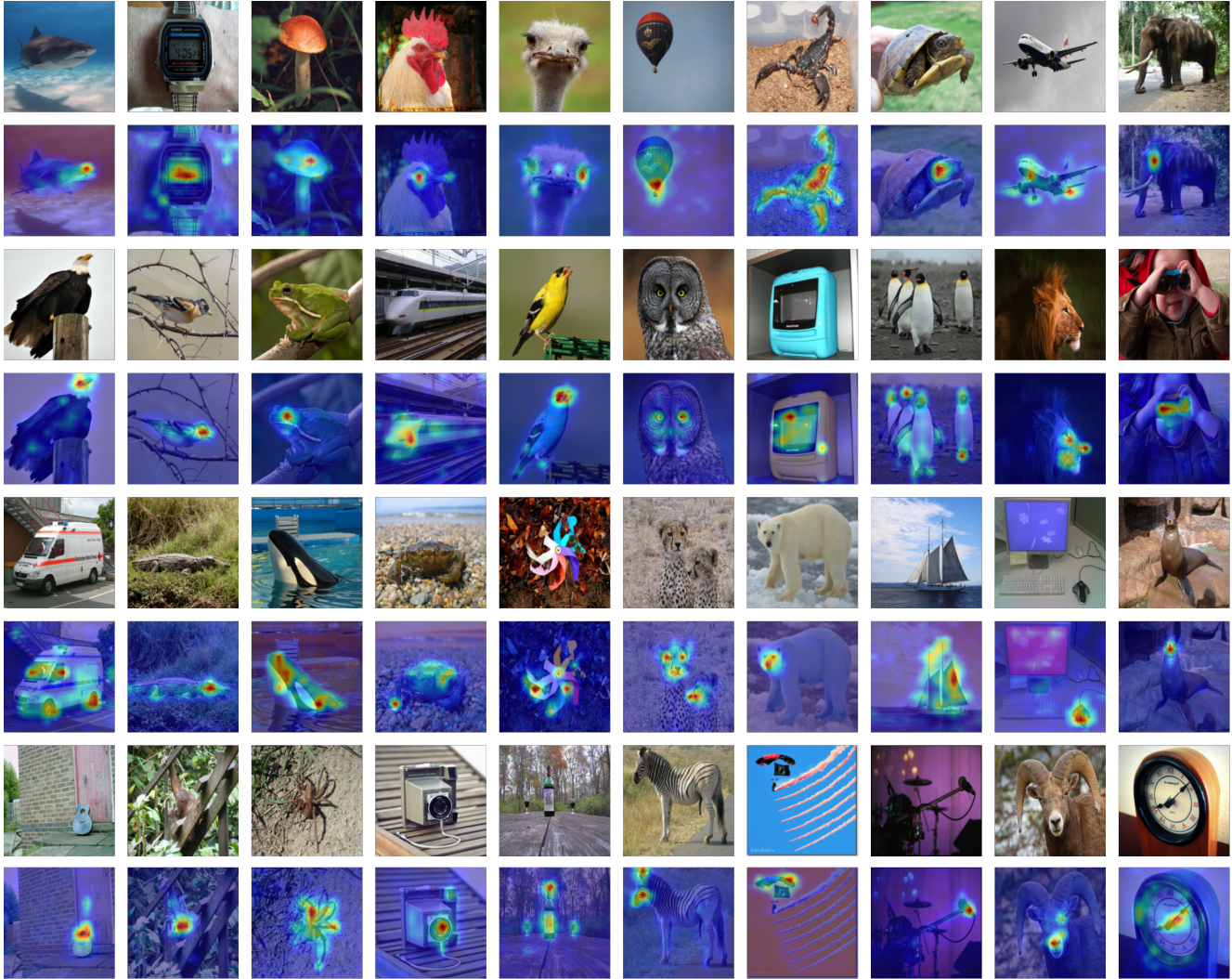


Figure 7. Attention visualization results of TT-T on ImageNet-1k dataset. We use the TT-T last layer attention map for visualization.

5. Conclusion

In this paper we propose a novel token transformer (TT), which is a simpler and more efficient one and can be used for multiple vision tasks. The core mechanism of TT is a long-range attention mechanism based on CLS tokens. It implements more efficient modeling of long-range dependencies without introducing additional layers or complex computational operations. In addition, the simple and intuitive design of SCFFN helps TT to enhance its modeling capabilities while handling two different nature tokens at the same time. In order to solve the problem that TT hierarchical design leads to the next stage CLS token cannot access the window information of the previous stage, we design FIM in each stage of TT. Ablation experiments have verified its effectiveness. The proposed TT achieves competitive results in several vision tasks. We hope that our

work will inspire the design of more efficient and simpler ways to model long range dependencies.

References

- [1] Moab Arar, Ariel Shamir, and Amit H Bermano. Learned queries for efficient local attention. In *Proceedings of the IEEE/CVF Conference on Computer Vision and Pattern Recognition*, pages 10841–10852, 2022. 2, 3, 6
- [2] Chun-Fu Chen, Rameswar Panda, and Quanfu Fan. Regionvit: Regional-to-local attention for vision transformers. *arXiv preprint arXiv:2106.02689*, 2021. 3
- [3] Chun-Fu Richard Chen, Quanfu Fan, and Rameswar Panda. Crossvit: Cross-attention multi-scale vision transformer for image classification. In *Proceedings of the IEEE/CVF international conference on computer vision*, pages 357–366, 2021. 1, 2

- [4] Xinlei Chen, Saining Xie, and Kaiming He. An empirical study of training self-supervised vision transformers. In *Proceedings of the IEEE/CVF International Conference on Computer Vision*, pages 9640–9649, 2021. 2
- [5] Xiangxiang Chu, Zhi Tian, Yuqing Wang, Bo Zhang, Haibing Ren, Xiaolin Wei, Huaxia Xia, and Chunhua Shen. Twins: Revisiting the design of spatial attention in vision transformers. *Advances in Neural Information Processing Systems*, 34:9355–9366, 2021. 1
- [6] Jia Deng, Wei Dong, Richard Socher, Li-Jia Li, Kai Li, and Li Fei-Fei. Imagenet: A large-scale hierarchical image database. In *2009 IEEE conference on computer vision and pattern recognition*, pages 248–255. Ieee, 2009. 2, 6
- [7] Mingyu Ding, Bin Xiao, Noel Codella, Ping Luo, Jingdong Wang, and Lu Yuan. Davit: Dual attention vision transformers. *arXiv preprint arXiv:2204.03645*, 2022. 3
- [8] Xiaoyi Dong, Jianmin Bao, Dongdong Chen, Weiming Zhang, Nenghai Yu, Lu Yuan, Dong Chen, and Baining Guo. Cswin transformer: A general vision transformer backbone with cross-shaped windows. In *Proceedings of the IEEE/CVF Conference on Computer Vision and Pattern Recognition*, pages 12124–12134, 2022. 3
- [9] Alexey Dosovitskiy, Lucas Beyer, Alexander Kolesnikov, Dirk Weissenborn, Xiaohua Zhai, Thomas Unterthiner, Mostafa Dehghani, Matthias Minderer, Georg Heigold, Sylvain Gelly, et al. An image is worth 16x16 words: Transformers for image recognition at scale. *arXiv preprint arXiv:2010.11929*, 2020. 1, 2, 6
- [10] Stéphane d’Ascoli, Hugo Touvron, Matthew L Leavitt, Ari S Morcos, Giulio Biroli, and Levent Sagun. Convit: Improving vision transformers with soft convolutional inductive biases. In *International Conference on Machine Learning*, pages 2286–2296. PMLR, 2021. 1
- [11] Benjamin Graham, Alaeldin El-Nouby, Hugo Touvron, Pierre Stock, Armand Joulin, Hervé Jégou, and Matthijs Douze. Levit: a vision transformer in convnet’s clothing for faster inference. In *Proceedings of the IEEE/CVF international conference on computer vision*, pages 12259–12269, 2021. 1
- [12] Ali Hassani and Humphrey Shi. Dilated neighborhood attention transformer. *arXiv preprint arXiv:2209.15001*, 2022. 3
- [13] Ali Hassani, Steven Walton, Nikhil Shah, Abulikemu Abuduweili, Jiachen Li, and Humphrey Shi. Escaping the big data paradigm with compact transformers. *arXiv preprint arXiv:2104.05704*, 2021. 2
- [14] Kaiming He, Georgia Gkioxari, Piotr Dollár, and Ross Girshick. Mask r-cnn. In *Proceedings of the IEEE international conference on computer vision*, pages 2961–2969, 2017. 6
- [15] Byeongho Heo, Sangdoon Yun, Dongyoon Han, Sanghyuk Chun, Junsuk Choe, and Seong Joon Oh. Rethinking spatial dimensions of vision transformers. In *Proceedings of the IEEE/CVF International Conference on Computer Vision*, pages 11936–11945, 2021. 2
- [16] Jinpeng Li, Yichao Yan, Shengcai Liao, Xiaokang Yang, and Ling Shao. Local-to-global self-attention in vision transformers. *arXiv preprint arXiv:2107.04735*, 2021. 3, 6
- [17] Wei Li, Xing Wang, Xin Xia, Jie Wu, Xuefeng Xiao, Min Zheng, and Shiping Wen. Sepvit: Separable vision transformer. *arXiv preprint arXiv:2203.15380*, 2022. 1
- [18] Yawei Li, Kai Zhang, Jie Zhang Cao, Radu Timofte, and Luc Van Gool. Localvit: Bringing locality to vision transformers. *arXiv preprint arXiv:2104.05707*, 2021. 1
- [19] Tsung-Yi Lin, Michael Maire, Serge Belongie, James Hays, Pietro Perona, Deva Ramanan, Piotr Dollár, and C Lawrence Zitnick. Microsoft coco: Common objects in context. In *European conference on computer vision*, pages 740–755. Springer, 2014. 2, 6
- [20] Ze Liu, Yutong Lin, Yue Cao, Han Hu, Yixuan Wei, Zheng Zhang, Stephen Lin, and Baining Guo. Swin transformer: Hierarchical vision transformer using shifted windows. In *Proceedings of the IEEE/CVF International Conference on Computer Vision*, pages 10012–10022, 2021. 1, 3, 6, 7
- [21] Zhuang Liu, Hanzi Mao, Chao-Yuan Wu, Christoph Feichtenhofer, Trevor Darrell, and Saining Xie. A convnet for the 2020s. In *Proceedings of the IEEE/CVF Conference on Computer Vision and Pattern Recognition*, pages 11976–11986, 2022. 6
- [22] Zizheng Pan, Jianfei Cai, and Bohan Zhuang. Fast vision transformers with hilo attention. *arXiv preprint arXiv:2205.13213*, 2022. 1
- [23] Zizheng Pan, Bohan Zhuang, Jing Liu, Haoyu He, and Jianfei Cai. Scalable vision transformers with hierarchical pooling. In *Proceedings of the IEEE/cvf international conference on computer vision*, pages 377–386, 2021. 1
- [24] Krushi Patel, Andres M Bur, Fengjun Li, and Guanghui Wang. Aggregating global features into local vision transformer. *arXiv preprint arXiv:2201.12903*, 2022. 3
- [25] Shitao Tang, Jiahui Zhang, Siyu Zhu, and Ping Tan. Quadtree attention for vision transformers. *arXiv preprint arXiv:2201.02767*, 2022. 1
- [26] Hugo Touvron, Matthieu Cord, Matthijs Douze, Francisco Massa, Alexandre Sablayrolles, and Hervé Jégou. Training data-efficient image transformers & distillation through attention. In *International Conference on Machine Learning*, pages 10347–10357. PMLR, 2021. 1, 7
- [27] Hugo Touvron, Matthieu Cord, Alexandre Sablayrolles, Gabriel Synnaeve, and Hervé Jégou. Going deeper with image transformers. In *Proceedings of the IEEE/CVF International Conference on Computer Vision*, pages 32–42, 2021. 1
- [28] Zhengzhong Tu, Hossein Talebi, Han Zhang, Feng Yang, Peyman Milanfar, Alan Bovik, and Yinxiao Li. Maxvit: Multi-axis vision transformer. *arXiv preprint arXiv:2204.01697*, 2022. 1
- [29] Cong Wang, Hongmin Xu, Xiong Zhang, Li Wang, Zhitong Zheng, and Haifeng Liu. Convolutional embedding makes hierarchical vision transformer stronger. In *European Conference on Computer Vision*, pages 739–756. Springer, 2022. 3
- [30] Wenhai Wang, Enze Xie, Xiang Li, Deng-Ping Fan, Kaitao Song, Ding Liang, Tong Lu, Ping Luo, and Ling Shao. Pyramid vision transformer: A versatile backbone for dense prediction without convolutions. In *Proceedings of the*

- IEEE/CVF International Conference on Computer Vision*, pages 568–578, 2021. 1, 3, 6
- [31] Wenxiao Wang, Lu Yao, Long Chen, Binbin Lin, Deng Cai, Xiaofei He, and Wei Liu. Crossformer: A versatile vision transformer hinging on cross-scale attention. *arXiv preprint arXiv:2108.00154*, 2021. 1
- [32] Haiping Wu, Bin Xiao, Noel Codella, Mengchen Liu, Xiyang Dai, Lu Yuan, and Lei Zhang. Cvt: Introducing convolutions to vision transformers. In *Proceedings of the IEEE/CVF International Conference on Computer Vision*, pages 22–31, 2021. 1, 2
- [33] Zhuofan Xia, Xuran Pan, Shiji Song, Li Erran Li, and Gao Huang. Vision transformer with deformable attention. In *Proceedings of the IEEE/CVF Conference on Computer Vision and Pattern Recognition*, pages 4794–4803, 2022. 2, 3, 6, 7
- [34] Tete Xiao, Yingcheng Liu, Bolei Zhou, Yuning Jiang, and Jian Sun. Unified perceptual parsing for scene understanding. In *Proceedings of the European conference on computer vision (ECCV)*, pages 418–434, 2018. 7
- [35] Jianwei Yang, Chunyuan Li, Pengchuan Zhang, Xiyang Dai, Bin Xiao, Lu Yuan, and Jianfeng Gao. Focal self-attention for local-global interactions in vision transformers. *arXiv preprint arXiv:2107.00641*, 2021. 2, 3, 6, 7
- [36] Hongxu Yin, Arash Vahdat, Jose M Alvarez, Arun Mallya, Jan Kautz, and Pavlo Molchanov. A-vit: Adaptive tokens for efficient vision transformer. In *Proceedings of the IEEE/CVF Conference on Computer Vision and Pattern Recognition*, pages 10809–10818, 2022. 1, 3
- [37] Fisher Yu, Vladlen Koltun, and Thomas Funkhouser. Dilated residual networks. In *Proceedings of the IEEE conference on computer vision and pattern recognition*, pages 472–480, 2017. 3
- [38] Li Yuan, Yunpeng Chen, Tao Wang, Weihao Yu, Yujun Shi, Zi-Hang Jiang, Francis EH Tay, Jiashi Feng, and Shuicheng Yan. Tokens-to-token vit: Training vision transformers from scratch on imagenet. In *Proceedings of the IEEE/CVF International Conference on Computer Vision*, pages 558–567, 2021. 2
- [39] Bolei Zhou, Hang Zhao, Xavier Puig, Tete Xiao, Sanja Fidler, Adela Barriuso, and Antonio Torralba. Semantic understanding of scenes through the ade20k dataset. *International Journal of Computer Vision*, 127(3):302–321, 2019. 2, 6
- [40] Daquan Zhou, Bingyi Kang, Xiaojie Jin, Linjie Yang, Xiaochen Lian, Zihang Jiang, Qibin Hou, and Jiashi Feng. Deepvit: Towards deeper vision transformer. *arXiv preprint arXiv:2103.11886*, 2021. 1, 2